Acta Universitatis Sapientiae
Electrical and Mechanical Engineering, 11 (2019) 67-78

DOI: 10.2478/auseme-2019-0006

A Four-Node Tetrahedral Finite Element Based on Space Fiber Rotation Concept

Kamel MEFTAH[1], Lakhdar SEDIRA[2]

[1] University of Biskra, Laboratoire de Génie Energétique et Matériaux, LGEM, Faculty of Sciences and Technology, Biskra, 07000, Algeria, e-mail: k.meftah@univ-biskra.dz
[2] University of Biskra, Laboratoire de Génie Mécanique, LGM, Faculty of Sciences and Technology, Biskra, 07000, Algeria, e-mail: l.sedira@univ-biskra.dz

Manuscript received August 23, 2019; revised September 19, 2019

Abstract: The paper presents a four-node tetrahedral solid finite element SFR4 with rotational degrees of freedom (DOFs) based on the Space Fiber Rotation (SFR) concept for modeling three-dimensional solid structures. This SFR concept is based on the idea that a 3D virtual fiber, after a spatial rotation, introduces an enhancement of the strain field tensor approximation. Full numerical integration is used to evaluate the element stiffness matrix. To demonstrate the efficiency and accuracy of the developed four-node tetrahedron solid element and to compare its performance with the classical four-node tetrahedral element, extensive numerical studies are presented.

Keywords: Four-node tetrahedral element, 3D finite element, Space Fiber Rotation concept, rotational DOFs.

1. Introduction

Three types of solid elements are commonly used in modeling three-dimensional solid structures: tetrahedron, hexahedron (also known as brick) and prism (also known wedge or pentahedron) elements. Because of their suitability for arbitrary complex geometries and fully automatic mesh generations, the use of tetrahedral elements becomes practically unavoidable in complex finite element structural analyses. Over the past two decades, there had been a revival of interest in the tetrahedral solid elements possessing rotational degrees of freedom (DOFs), to improve the computational efficiency of the standard first-order elements. Various formulations have been used for the development of tetrahedral finite elements with rotational degrees of freedom. One of the first achievements in this direction was due to Pawlak et al. [1] in the development of the 4-node tetrahedral element, including translations and rotations as nodal

DOFs for 3D elasticity problems. In the work of Sze and Pan [2], a hybrid stress tetrahedron element with Allmans rotation DOFs is developed. Stabilization techniques are used to control the spurious modes by the four skew symmetric stress modes. It is interesting to note that the advanced 4-node elements with only corner nodes and rotational DOFs are obtained from that a subparametric 10-node tetrahedron element. Another simple approach to construct a 4-node tetrahedron element with rotational DOFs has been proposed by Matsubara et al. [3]. Working along the lines of rotational DOFs framework, Tian and Yagawa [4] developed a 4-node quadratic tetrahedron element with four corner nodes using the generalized node following the idea of the partition-of-unity-based finite element approximation. Later, Tian et al. [5] published the work on advanced 4-node tetrahedron elements using vertex rotational DOFs. It is noteworthy that the accuracy of their solid elements is significantly better than the accuracy of the classical first-order elements and globally close to that of the classical quadratic elements. A description of other available theories can be found, for example, in the review article by Tian et al. [6]. Also, in Reference [7] various elements are described that add rotational degrees of freedom to a four-node tetrahedron with the rotational formulation generally based on assumed strains or displacement gradients of a ten node tetrahedron.

The so-called Space Fiber Rotation (SFR) concept was firstly introduced by Ayad [8] and later by Meftah [9] to enhance the accuracy of first-order finite elements. This SFR concept was then adapted to 3D elastic structures by Meftah et al. [10] by developing a 3D six-node prismatic solid element, named SFR6, and by Ayad et al. [11] by introducing two 3D eight-node hexahedral solid elements named SFR8 and SFR8I (with incompatible mode). One would like to recall that the present concept was firstly derived from 2D and extended later for 3D virtual rotations of a nodal fiber that improves the approximation of the displacement vector. These SFR concept-based solid elements present three rotational and three translational DOFs per node. Furthermore, in the work of Meftah et al. [12], an extension of the SFR eight-node hexahedral elements SFR8 and SFR8I, was proposed to account for geometrically nonlinear problems. Moreover, Meftah et al. [13] developed a multilayered extension of the eight-node hexahedral element named SFR8M to study composite laminate structures. In particular, it was shown that these 3D SFR solid elements yield results that are significantly better than those of the classical first-order wedge and hexahedral elements and globally close to those of the classical quadratic elements. It should be noted that the SFR solid elements maintain a good performance especially for coarse and distorted meshes [9-14].

In this work, we present a four-node tetrahedral solid finite element SFR4 to study full three-dimensional solid structures. Hence, the element has six DOFs per node, i.e. three displacements and three rotational parameters. The proposed tetrahedral element is developed by exploiting the concept of Space Fiber Rotation. These terms, represented by the fictitious rotational degrees of freedom, would result in the creation of an interesting added value by providing a reliable and accurate solution. The intent is to introduce a four-node tetrahedral element that is computationally attractive when compared with the classical four-node tetrahedral element with translations only as DOFs. This element uses an exact integration scheme with four-point rule. Their performances are investigated by studying several solid structures.

2. The SFR concept finite element approximation

The SFR concept is based on the space rotation of a virtual fiber. *Fig. 1* shows the geometry of the four-node tetrahedral element, in which a virtual space fiber $\underline{iq}$ is incorporated at the nodal level. The fiber rotation, represented by the rotation vector $\underline{\theta}$, will generate an additional displacement vector that would enrich the classical displacement field $\underline{U}_q$ of point q, used to formulate the standard 4-node solid tetrahedral element [10, 11].

$$\underline{U}(\xi,\eta,\zeta) = \sum_{i=1}^{4} N_i\,(\xi,\eta,\zeta)\left(\underline{U}_i + \underline{\theta}_i \wedge \underline{iq}\right);\ \underline{U}_q \equiv \underline{U}\ , \tag{1}$$

where $\{\underline{U}_i\} = \{U_i, V_i, W_i\}^T$ is the nodal displacement vector and N_i are the classical interpolation functions associated with the classical four-node tetrahedral element given by:

$$[N] = [1-\xi-\eta-\zeta \quad \xi \quad \eta \quad \zeta], \tag{2}$$

where ξ, η and $\zeta \in [0,1]$ with $1-\xi-\eta-\zeta \geq 0$.

In addition

$$\{iq\} = \begin{Bmatrix} x - x_i \\ y - y_i \\ z - z_i \end{Bmatrix};\ \{\theta_i\} = \begin{Bmatrix} \theta_{xi} \\ \theta_{yi} \\ \theta_{zi} \end{Bmatrix}, \tag{3}$$

where (x_i, y_i, z_i) are the Cartesian coordinates of node i, and (x, y, z) are the Cartesian coordinates of any point q of the element SFR4 given by the following approximations:

$$x = \sum_{i=1}^{4} N_i x_i\ ;\ y = \sum_{i=1}^{4} N_i y_i\ ;\ z = \sum_{i=1}^{4} N_i z_i\ . \tag{4}$$

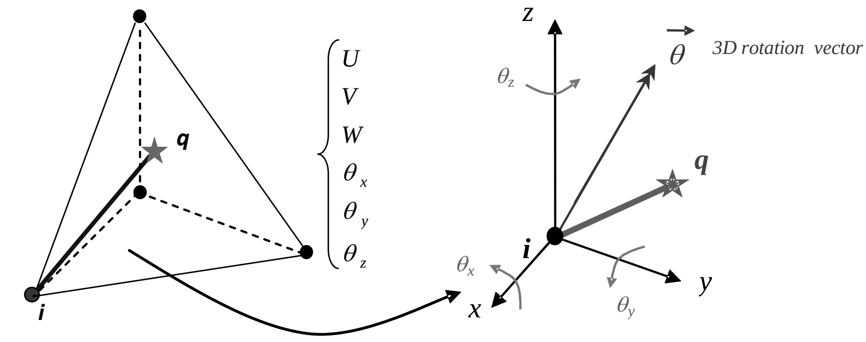

a. Four-node tetrahedral element SFR 4 b. Space fiber *iq*

Figure 1: Geometry and kinematics of a virtual space fiber (SFR approach).

By performing the vector product $\underline{\theta}_i \wedge \underline{iq}$, we obtain the following approximation:

$$\{U\}=[N]\{U_n^e\}\ ;\ [N]=\begin{bmatrix} & [N_{Ui}] & \\ \cdots & [N_{Vi}] & \cdots \\ & [N_{Wi}] & \end{bmatrix};\ i=1,\ldots,4, \tag{5}$$

where

$$\begin{aligned} [N_{Ui}] &= [\,N_i \quad 0 \quad 0 \quad 0 \quad N_i(z-z_i) \quad -N_i(y-y_i)\,] \\ [N_{Vi}] &= [\,0 \quad N_i \quad 0 \quad -N_i(z-z_i) \quad 0 \quad N_i(x-x_i)\,] \\ [N_{Wi}] &= [\,0 \quad 0 \quad N_i \quad N_i(y-y_i) \quad -N_i(x-x_i) \quad 0\,] \end{aligned} \tag{6}$$

and

$$\{u_n^e\}=\{\cdots \quad U_i \quad V_i \quad W_i \quad \theta_{xi} \quad \theta_{yi} \quad \theta_{zi} \quad \cdots\}^T;\ i=1,\ldots,4 \tag{7}$$

is the nodal degrees of freedom vector of SFR4 element containing three translational and three fictive rotational DOFs per node, see *Fig. 1(a)* [10], [11].

The strain tensor of any point q is classically defined in the global coordinate system by:

$$\varepsilon_{xx}=U_{,x}\ ;\ \varepsilon_{yy}=V_{,y}\ ;\ \varepsilon_{zz}=W_{,z}\ ;\ \gamma_{xy}=2\varepsilon_{xy}=U_{,y}+V_{,x} \tag{8.a}$$

$$\gamma_{xz}=2\varepsilon_{xz}=U_{,z}+W_{,x}\ ;\ \gamma_{yz}=2\varepsilon_{yz}=V_{,z}+W_{,y}\,. \tag{8.b}$$

Using expressions Eq. (8) of the mechanical strains and the approximation Eq. (5) of the displacement vector, we obtain a matrix relationship between the stain vector $\{\varepsilon\}$ and the nodal degrees of freedom vector $\{U_n\}$:

$$\{\varepsilon\} = [B]\{U_n\} \ ; \ \underbrace{[B]}_{6\times 24} = \begin{bmatrix} \{N_{U,x}\}^T \\ \{N_{V,y}\}^T \\ \{N_{W,z}\}^T \\ \{N_{U,y}\}^T + \{N_{V,x}\}^T \\ \{N_{U,z}\}^T + \{N_{W,x}\}^T \\ \{N_{V,z}\}^T + \{N_{W,y}\}^T \end{bmatrix}, \tag{9}$$

where

$$\begin{aligned} \lfloor N_{\alpha,x} \rfloor &= j_{11}\lfloor N_{\alpha,\xi} \rfloor + j_{12}\lfloor N_{\alpha,\eta} \rfloor + j_{13}\lfloor N_{\alpha,\zeta} \rfloor \\ \lfloor N_{\alpha,y} \rfloor &= j_{21}\lfloor N_{\alpha,\xi} \rfloor + j_{22}\lfloor N_{\alpha,\eta} \rfloor + j_{23}\lfloor N_{\alpha,\zeta} \rfloor \quad ; \quad \alpha \equiv U,V,W \\ \lfloor N_{\alpha,z} \rfloor &= j_{31}\lfloor N_{\alpha,\xi} \rfloor + j_{32}\lfloor N_{\alpha,\eta} \rfloor + j_{33}\lfloor N_{\alpha,\zeta} \rfloor \end{aligned} \tag{10}$$

and j_{lk} are the inverse Jacobian matrix components.

For linear elastic problems, the stiffness matrix of SFR4 takes the following simple form:

$$\left[K^e\right] = \int_0^1 \int_0^{1-\zeta} \int_0^{1-\eta-\zeta} \left([B]^T [C][B] DetJ\right)_{\xi,\eta,\zeta} d\xi d\eta d\zeta = \sum_{i=1}^{Npi} w_i \left([B]^T [C][B] DetJ\right)_{\xi_i,\eta_i,\zeta_i} , \tag{11}$$

where $[C]$ is the elasticity matrix relating the stress and strain vectors and N_{pi} is the number of integration points. For a homogeneous and isotropic material this matrix for a three-dimensional problem can be written as:

$$[C] = \begin{bmatrix} 2G+\lambda & \lambda & \lambda & 0 & 0 & 0 \\ \lambda & 2G+\lambda & \lambda & 0 & 0 & 0 \\ \lambda & \lambda & 2G+\lambda & 0 & 0 & 0 \\ 0 & 0 & 0 & G & 0 & 0 \\ 0 & 0 & 0 & 0 & G & 0 \\ 0 & 0 & 0 & 0 & 0 & G \end{bmatrix}. \tag{12}$$

The Lamé coefficients are expressed in terms of Young's modulus, E, and Poisson's ratio, ν, by:

$$\lambda = \frac{E\nu}{(1+\nu)(1-2\nu)} \text{ and } G = \frac{E}{2(1+\nu)} . \tag{13}$$

The approximation of the part corresponding to the rotation of space fiber is quadratic in terms of ξ, η and ζ. The element stiffness matrix is integrated exactly using a four-point numerical quadrature (N_{pi} = 4) [15].

3. Numerical examples

In this section, we present various three-dimensional benchmark problems, selected from the literature, have been used to evaluate the performance and convergence rate of the proposed four-node tetrahedral solid element SFR4.

A. Cantilever beam

Fig. 2 shows a cantilever benchmark problem used in convergence study by Tian et al. [4]. The material parameters are: Young's modulus is $E = 3.1\times10^7$ N/cm^2 and the Poisson's ratio is $\nu = 0.3$. The exact solution of deflection (v_{exact}) at the center point of the free end is given by Timoshenko and Goodier [16]:

$$v_{exact} = \frac{P}{6EI}\left[3\nu\left(y-\frac{H}{2}\right)^2(L-x)+\frac{1}{4}(4+5\nu)H^2x+(3L-x)x^2\right] \tag{14}$$

The displacements in the directions of the applied loads are computed and normalized with respect to the exact solutions of (14). *Table 1* presents the convergence of the normalized tip deflection (v_{num}/v_{exact}) at the center point of the free end. Obviously, the present element appeared to be the better performer compared to the classical first-order Tet4 element taken from Reference [1].

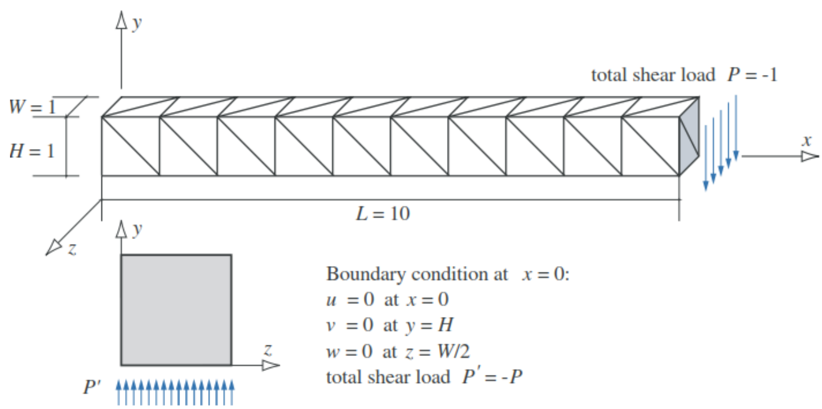

Figure 2: The cantilever benchmark problem used in convergence study, a 10×1×1 mesh is shown; a brick is disassembled into six tetrahedrons (W = 1 *cm*, H = 1 *cm*, L = 10 *cm* and P = −1 *N*).

Table 1: Normalized tip deflection ratios for the cantilever problem (v_{num}/v_{exact})

Mesh	Tet4	SFR4
10×1×1	0.247	0.576
20×2×2	0.531	0.734
30×4×4	0.803	0.923
40×8×8	0.939	0.992

B. In-plane bending of a cantilever beam

Fig. 3 shows the geometry, boundary conditions and material properties of a cantilever beam subjected to a plane transverse bending load. A reference analytic solution of the transverse displacement of point C, belonging to the beam's end face, is obtained using the Timoshenko beam theory: $V_{ref}^{C} = 4.03$ *mm*. This cantilever beam is modeled with six meshes: three regular meshes M1, M2 and M3 and three distorted ones M4, M5 and M6 as shown in *Fig. 4* (a brick element is disassembled into six tetrahedral elements). We summarize in *Table 2* the normalized transverse displacement results. These numerical results show that the four-node tetrahedral SFR4 element is sensitive to mesh distortion. We also remark that SFR4 results are better than those of the non-rotational standard four-node tetrahedral element Tet4.

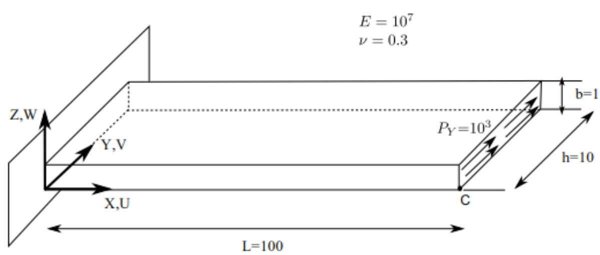

Figure 3: Plane bending of a thin cantilever beam ($E = 10^7$ MPa, $\nu = 0.3$, L = 100 *mm*, b = 1 *mm*, h = 10 *mm* and $P_Y = 10^3$ *N*).

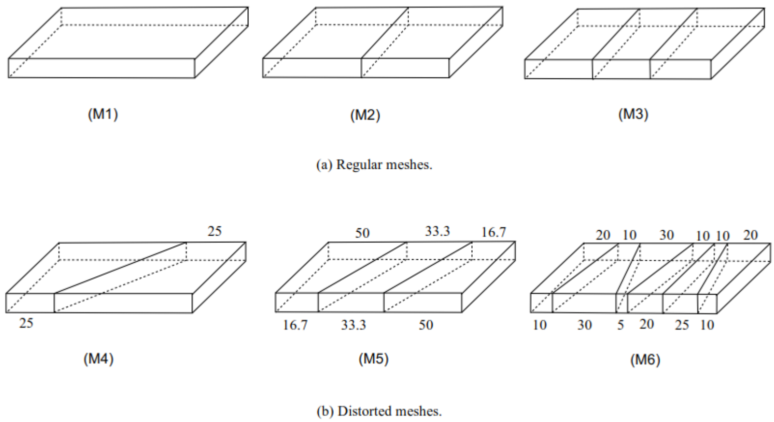

Figure 4: Plane bending of a cantilever beam. 3D meshing.

Table 2: In-plane bending of a cantilever beam. Normalized transverse displacement of point C

Mesh	Tet4	SFR4
M1	0.012	0.060
M2	0.034	0.221
M3	0.064	0.382
M4	0.014	0.110
M5	0.024	0.161
M6	0.058	0.306

C. Straight cantilever beam

The straight cantilever beam test proposed by MacNeal and Harder [17] also investigates sensitivity to mesh distortion in bending. The beam is meshed with six elements (where a brick is disassembled into six tetrahedrons) and subjected to unit-shear force at free end (*Fig. 5*). The elements are distorted from regular bricks to parallelogram-shaped elements. Geometries, material properties and loading of straight cantilever beams are defined in *Fig. 5*. The theoretical solutions for beam problems obtained from MacNeal and Harder [17] are summarized in *Table 3*. The normalized tip deflection results are summarized in *Table 4*. These numerical results are always more accurate than the first-order tetrahedral element Tet4 in all mesh configurations.

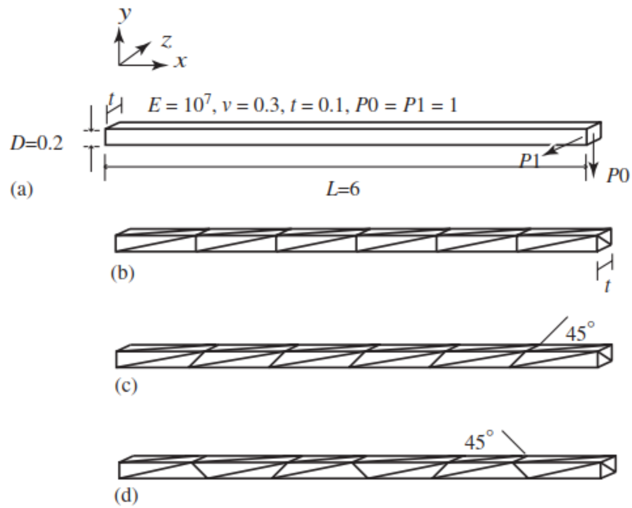

Figure 5: Straight cantilever beam: (a) geometry and material parameters; (b) regular mesh; (c) parallelogram mesh; (d) trapezoid mesh ($E = 10^7$ N/cm^2, $\nu = 0.3$, $L = 6$ cm, $t = 0.1$ cm, $D = 0.2$ cm and $P_0 = P_1 = 1$ N).

Table 3: Theoretical solutions for beam problems

Tip load direction	Straight beam	Curved beam
In-plane shear	0.1081 (*cm*)	0.08734 (*cm*)
Out-of-plane shear	0.4321 (*cm*)	0.5022 (*cm*)

Table 4: Normalized tip deflection of the straight cantilever beam

Element shape	Load type	Tet4	SFR4
Regular	In-plane	0.010	0.053
	Out-of-plane	0.012	0.064
Trapezoidal	In-plane	0.006	0.032
	Out-of-plane	0.007	0.037
Parallelogram	In-plane	0.010	0.054
	Out-of-plane	0.007	0.038

D. Curved beam

The curved beam is portrayed in *Fig. 6*. This figure shows the geometry, meshes and material properties. All nodal DOFs at the clamped end are restrained. At the free end, in-plane and out-of-plane forces are applied. The displacements at the free end in the directions of the forces are computed and normalized by the reference solution of MacNeal and Harder [17] reported in *Table 3*. The normalized end deflections in the loading directions are tabulated in *Table 5*. Superior accuracy of the SFR4 element over the standard 4-node tetrahedral element can be observed.

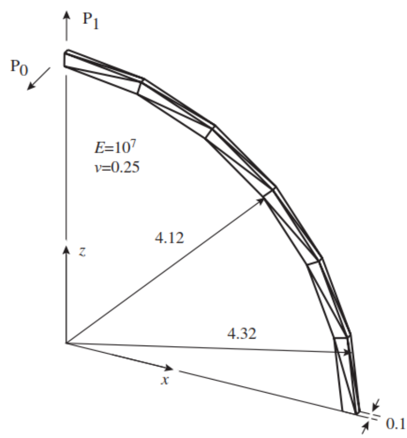

Figure 6: Curved cantilever beam loaded with an in-plane P_1 and out-of-plane P_0 shear load ($E = 10^7$ N/cm^2, $\nu = 0.25$, $R_{int} = 4.12$ cm, $R_{ext} = 4.32$ cm and $P_0 = P_1 = 1$ N).

Table 5: Normalized end deflection of the curved beam

Load type	Tet4	SFR4
In-plane	0.023	0.092
Out-of-plane	0.005	0.121

E. Twisted beam

The clamped thick twisted beam proposed by MacNeal and Harder [17], under in-plane and out-of-plane unit loading ($P = 1$ N) at its free end, is analyzed. This test and the mesh are presented in *Fig. 7*. All the displacements at the clamped end are restrained. The theoretical solutions for displacements in the directions of the applied loads to the problems are [17]: 0.005424 *cm* for in-plane loading and 0.001754 *cm* for out-of-plane loading. The normalized results with respect to the theoretical solutions of MacNeal and Harder [17] are summarized in *Table 6*. Again, the new element presented in this paper using SFR possesses the better performance compared with the classical 4-node tetrahedral element.

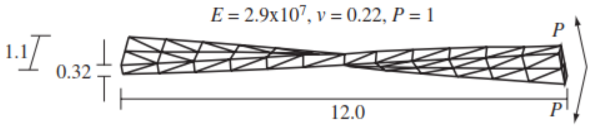

Figure 7: Twisted beam subjected to unit in-plane force and out-of-plane force (E = 2.9×10^7 N/cm^2, ν = 0.22, L= 12 cm, b = 1.1 cm, h = 0.32 cm and P = 1 N).

Table 6: Normalized displacements in the loading directions for the twisted cantilever beam problem

Tip load direction	Tet4	SFR4
In-plane loading	0.096	0.234
Out-of-plane loading	0.080	0.271

4. Summary and conclusions

In this paper, a new four-node tetrahedral solid element SFR4 with six DOFs (three translations and three rotations) per node based on the Space Fiber Rotation concept is presented. This concept considers the 3D rotation of a virtual fiber that improves the displacement field by additional terms incorporated in any classical first-order elements. Numerical results show that the proposed four-node tetrahedral element SFR4 provides further improvement to the classical first-order four-node tetrahedral element Tet4, which is fully reflected in the analysis of three-dimensional elastic problems. In addition, the SFR concept is shown to be an efficient tool for developing high accuracy elements. As a future work, the reduced integration rule with one-point will be tested in SFR4 element to prevent some locking phenomena and to enhance computational efficiency.

References

[1] Pawlak, T. P., Yunus, S. M. and Cook, R. D., "Solid elements with rotational degrees of freedom: Part II–tetrahedron elements", *International Journal for Numerical Methods in Engineering*, 31, 593–610, 1991. doi.org/10.1002/nme.1620310311.

[2] Sze, K. and Pan, Y., “Hybrid stress tetrahedral elements with Allman’s rotational DOFs”, *International journal for numerical methods in engineering*, 48, 1055–1070, 2000. doi.org/10.1002/(SICI)1097-0207(20000710)48:7<1055::AID-NME916>3.0.CO;2-P

[3] Matsubara, H., Iraha, S., Tomiyama, J., Yamashiro, T., and Yagawa, G. “Free mesh method using tetrahedral element including the vertex rotations”, *in*: *Proceedings-Japan Society of Civil Engineers*, DOTOKU GAKKAI, pp. 97–108, 2004.

[4] Tian, R. and Yagawa, G., “Generalized nodes and high-performance elements”, *International Journal for Numerical Methods in Engineering*, 64, 2039–2071, 2005. doi.org/10.1002/ nme.1436.

[5] Tian, R., Matsubara, H. and Yagawa, G., “Advanced 4-node tetrahedrons”, *International Journal for Numerical Methods in Engineering*, 68, 1209–1231, 2006. doi.org/10.1002/ nme.1744

[6] Tian, R., Matsubara, H., Yagawa, G., Iraha, S. and Tomiyama, J., “Accuracy improvements on free mesh method: A high performance quadratic triangular/tetrahedral element with only corners”, *in*: *Proc. of the Sixth World Congress on Computational Mechanics* (WCCM VI), 2004.

[7] Hua, X. and To, C., “Simple and efficient tetrahedral finite elements with rotational degrees of freedom for solid modeling”, *Journal of Computing and Information Science in Engineering*, 7, 382–393, 2007. doi:10.1115/1.2798120.

[8] Ayad, R., “Contribution à la Modélisation numérique pour l’analyse des solides et des structures, et pour la mise en forme des fluides non newtoniens. Application à des matériaux d’emballage [Contribution to the numerical modeling of solids and structures and the non-Newtonian fluids forming process. Application to packaging materials]”, Habilitation to conduct researches, University of Reims, Reims, France, (in French), 2002.

[9] Meftah, K., “Modélisation numérique des solides par éléments finis volumiques basés sur le concept SFR [Numerical modeling of 3D structure by solid finite elements based upon the SFR concept] (Space Fiber Rotation)”, PhD thesis, University of Biskra, Algeria, (in French), 2013.

[10] Meftah, K., Ayad, R. and Hecini, M., “A new 3D 6-node solid finite element based upon the “Space Fibre Rotation” concept”, *European Journal of Computational Mechanics*, 22, 1-29, 2012. doi.org/10.1080/17797179.2012.721502.

[11] Ayad, R., Zouari, W., Meftah, K., Zineb, T. B., and Benjeddou, A., “Enrichment of linear hexahedral finite elements using rotations of a virtual space fiber”, *International Journal for Numerical Methods in Engineering*, 95, 46-70, 2013. doi.org/10.1002/nme.4500.

[12] Meftah, K., Zouari, W., Sedira, L. and Ayad, R., “Geometric non-linear hexahedral elements with rotational DOFs”, *Computational Mechanics*, 57, 37-53, 2016. doi.org/10.1007/s00466-015-1220-8.

[13] Meftah, K., Sedira, L., Zouari, W., Ayad, R., and Hecini, M., “A multilayered 3D hexahedral finite element with rotational DOFs”, *European Journal of Computational Mechanics*, 24, 107-28, 2015. doi.org/10.1080/17797179.2015.1089462.

[14] Zouari, W., Assarar, M., Meftah, K. and Ayad, R., “Free vibration analysis of homogeneous piezoelectric structures using specific hexahedral elements with rotational DOFs”, *Acta Mechanica*, 226, 1737-56, 2015. doi.org/10.1007/s00707-014-1274-2.

[15] Dhondt, G. D. C., “The finite element method for three-dimensional thermomechanical applications”, John Wiley & Sons Inc, 2004.

[16] Timoshenko, S. P. and Goodier, J. N., “Theory of Elasticity”, 3rd edition, McGraw-Hill, New York, 1970.

[17] MacNeal, R. H., and Harder, R. L., “A proposed standard set of problems to test finite element accuracy”, *Finite Elements in Analysis and Design*, 1, 3–20, 1985. doi.org/ 10.1016/0168-874X(85)90003-4.